Purely irrotational theories of the effect of the viscosity on the decay of free gravity waves

By J. WANG AND D. D. JOSEPH

Department of Aerospace Engineering and Mechanics, Unversity of Minnesota,
Minneapolis, MN 55455, USA

It is generally believed that the major effects of viscosity are associated with vorticity. This belief is not always well founded; major effects of viscosity can be obtained from purely irrotational analysis of flows of viscous fluids. Here we illustrate this point by comparing our irrotational solutions with Lamb's 1932 exact solution of the problem of the decay of free gravity waves. Excellent agreements, even in fluids 10^7 more viscous than water, are achieved for the decay rates $n(k)$ for all wavenumbers k, excluding a small interval around a critical value k_c where progressive waves change to monotonic decay.

1. Introduction

Lamb (1932, §§ 348, 349) performed an analysis of the effect of viscosity on free gravity waves. He computed the decay rate by a dissipation method using the irrotational flow only. He also constructed an exact solution for this problem, which satisfies both the normal and shear stress conditions at the interface.

Joseph & Wang (2004) studied Lamb's problem using the theory of viscous potential flow (VPF) and obtained a dispersion relation which gives rise to both the decay rate and wave-velocity. They also computed a viscous correction for the irrotational pressure and used this pressure correction in the normal stress balance to obtain another dispersion relation. This method is called a viscous correction of the viscous potential flow (VCVPF). Since VCVPF is an irrotational theory, the shear stress cannot be made to vanish. However, the shear stress in the energy balance can be eliminated in the mean by the selection of an irrotational pressure which depends on viscosity.

Here we find that the viscous pressure correction gives rise to a higher-order irrotational correction to the velocity, which is proportional to the viscosity and does not have a boundary-layer structure. The corrected velocity depends strongly on viscosity and is not related to vorticity. The corrected irrotational flow gives rise to a dispersion relation which is in splendid agreement with Lamb's exact solution, which has no explicit viscous pressure. The agreement with the exact solution holds for fluids even 10^7 times more viscous than water and for all wavenumbers away from the cutoff wavenumber k_c which marks the place where progressive waves change to monotonic decay. We find that VCVPF gives rise to the same decay rate as in Lamb's exact solution and in his dissipation calculation when $k < k_c$. The exact solution agrees with VPF when $k > k_c$. The effects of vorticity are evident only in a small interval centred on the cutoff wavenumber. We present a comprehensive comparison for the decay rate and wave-velocity given by Lamb's exact solution and Joseph & Wang's VPF and VCVPF theories.

2. Irrotational viscous corrections for the potential flow solution

The gravity wave problem is governed by the linearized Navier–Stokes equation and the continuity equation

$$\frac{\partial \boldsymbol{u}}{\partial t} = -\frac{1}{\rho}\nabla p - g\boldsymbol{e}_y + \nu\nabla^2\boldsymbol{u}, \tag{2.1}$$

$$\nabla \cdot \boldsymbol{u} = 0, \tag{2.2}$$

subject to the boundary conditions at the free surface $(y \approx 0)$

$$T_{xy} = 0, \quad T_{yy} = 0, \tag{2.3}$$

where T_{xy} and T_{yy} are components of the stress tensor and the surface tension is neglected. Surface tension is important at high wavenumbers but, for simplicity, is neglected in the analyses given here. We divide the velocity and pressure field into two parts

$$\boldsymbol{u} = \boldsymbol{u}_p + \boldsymbol{u}_v, \quad p = p_p + p_v, \tag{2.4}$$

where the subscript p denotes potential solutions and v denotes viscous corrections. The potential solutions satisfy

$$\boldsymbol{u}_p = \nabla\phi, \quad \nabla^2\phi = 0, \tag{2.5}$$

and

$$\frac{\partial \boldsymbol{u}_p}{\partial t} = -\frac{1}{\rho}\nabla p_p - g\boldsymbol{e}_y. \tag{2.6}$$

The viscous corrections are governed by

$$\nabla \cdot \boldsymbol{u}_v = 0, \tag{2.7}$$

$$\frac{\partial \boldsymbol{u}_v}{\partial t} = -\frac{1}{\rho}\nabla p_v + \nu\nabla^2\boldsymbol{u}_v. \tag{2.8}$$

We take the divergence of (2.8) and obtain

$$\nabla^2 p_v = 0, \tag{2.9}$$

which shows that the pressure correction must be harmonic. Next we introduce a streamfunction ψ so that (2.7) is satisfied identically:

$$u_v = -\frac{\partial \psi}{\partial y}, \quad v_v = \frac{\partial \psi}{\partial x}. \tag{2.10}$$

We eliminate p_v from (2.8) by cross-differentiation and obtain the following equation for the streamfunction

$$\frac{\partial}{\partial t}\nabla^2\psi = \nu\nabla^4\psi. \tag{2.11}$$

To determine the normal modes which are periodic in respect of x with a prescribed wavelength $\lambda = 2\pi/k$, we assume that

$$\psi = B\mathrm{e}^{nt+ikx}\mathrm{e}^{my}, \tag{2.12}$$

where m is to be determined from (2.11). Inserting (2.12) into (2.11), we obtain

$$(m^2 - k^2)[n - \nu(m^2 - k^2)] = 0. \tag{2.13}$$

The root $m^2 = k^2$ gives rise to irrotational flow; the root $m^2 = k^2 + n/\nu$ leads to the rotational component of the flow. The rotational component cannot give rise to a

harmonic pressure satisfying (2.9) because

$$\nabla^2 e^{nt+ikx} e^{my} = (m^2 - k^2) e^{nt+ikx} e^{my} \tag{2.14}$$

does not vanish if $m^2 \neq k^2$. Thus, the governing equation for the rotational part of the flow can be written as

$$\frac{\partial \psi}{\partial t} = \nu \nabla^2 \psi. \tag{2.15}$$

This is the equation used by Lamb (1932) for the rotational part of his exact solution.

The effect of viscosity on the decay of a free gravity wave can be approximated by a purely irrotational theory in which the explicit appearance of the irrotational shear stress in the mechanical energy equation is eliminated by a viscous contribution p_v to the irrotational pressure. In this theory $\boldsymbol{u} = \nabla \phi$ and a streamfunction, which is associated with vorticity, is not introduced. The kinetic energy, potential energy and dissipation of the flow can be computed using the potential flow solution

$$\phi = A e^{nt+ky+ikx}. \tag{2.16}$$

We insert the potential flow solution into the mechanical energy equation

$$\frac{\mathrm{d}}{\mathrm{d}t} \left(\int_V \rho |\boldsymbol{u}|^2 / 2 \, \mathrm{d}V + \int_0^\lambda \rho g \eta^2 / 2 \, \mathrm{d}x \right) = \int_0^\lambda [v(-p + \tau_{yy}) + u \tau_{xy}] \, \mathrm{d}x + \int_V 2\mu \boldsymbol{D} : \boldsymbol{D} \, \mathrm{d}V, \tag{2.17}$$

where η is the elevation of the surface and $\boldsymbol{D}$ is the rate of strain tensor. Motivated by previous authors (Moore 1963; Kang & Leal 1988), we add a pressure correction to the normal stress which satisfies

$$\int_0^\lambda v(-p_v) \, \mathrm{d}x = \int_0^\lambda u \tau_{xy} \, \mathrm{d}x. \tag{2.18}$$

However, in our problem here, there is no explicit viscous pressure function in the exact solution (see (3.1) and (3.2)). It turns out that the pressure correction defined here in the purely irrotational flow is related to quantities in the exact solution in a complicated way which requires further analysis (see (3.8)).

Joseph & Wang (2004) solved for the harmonic pressure correction from (2.9), then determined the constant in the expression of p_v using (2.18), and obtained

$$p_v = -2\mu k^2 A e^{nt+ky+ikx}. \tag{2.19}$$

The velocity correction associated with this pressure correction can be solved from (2.8). We seek normal modes solution $\boldsymbol{u}_v \sim e^{nt+ky+ikx}$ and equation (2.8) becomes

$$\rho n \boldsymbol{u}_v = -\nabla p_v. \tag{2.20}$$

Hence, $\mathrm{curl}(\boldsymbol{u}_v) = 0$ and $\boldsymbol{u}_v$ is irrotational. After assuming $\boldsymbol{u}_v = \nabla \phi_1$ and $\phi_1 = A_1 e^{nt+ky+ikx}$, we obtain

$$\rho n \phi_1 = -p_v \Rightarrow \phi_1 = \frac{2\mu k^2}{\rho n} A e^{nt+ky+ikx}. \tag{2.21}$$

We compute the viscous normal stress due to the velocity correction

$$2\mu \frac{\partial v_v}{\partial y} = 2\mu \frac{\partial^2 \phi_1}{\partial y^2} = \frac{4\mu^2 k^4}{\rho n} A e^{nt+ky+ikx}. \tag{2.22}$$

Since for mobile fluids such as water or even glycerine, $\nu = \mu/\rho$ is small, this viscous normal stress is negligible compared to p_v when k is small. Therefore, the viscous normal stress induced by the velocity correction can be neglected in the normal stress balance in the VPVPF theory. The viscous normal stress (2.22) could be large when k is large; however, we will show in the following sections that the flow is nearly irrotational at large values of k and no correction is required.

This calculation shows that the velocity $\boldsymbol{u}_v$ associated with the pressure correction is irrotational. The pressure correction (2.19) is proportional to μ and it induces a correction ϕ_1 given by (2.21), which is also proportional to μ. The shear stress computed from $\boldsymbol{u}_v = \nabla\phi_1$ is then proportional to μ^2. To balance this non-physical shear stress, we can add a pressure correction proportional to μ^2, which will in turn induce a correction for the velocity potential proportional to μ^2. We can continue to build higher-order corrections and they will all be irrotational. The final velocity potential has the following form

$$\phi = (A + A_1 + A_2 + \cdots)\mathrm{e}^{nt+ky+\mathrm{i}kx}, \tag{2.23}$$

where $A_1 \sim \mu$, $A_2 \sim \mu^2 \dots$. Thus, the VCVPF theory is an approximation to the exact solution based on solely potential flow solutions. The higher-order corrections are small for liquids with small viscosities; the most important correction is the first pressure correction proportional to μ. In our application of VCPVF to the gravity wave problem, only the first pressure correction (2.19) is added to the normal stress balance and higher-order normal stress terms such as (2.22) are not added. We obtain a dispersion relation in excellent agreement with Lamb's exact solution (see the comparison in the next section); adding the higher-order corrections to the normal stress balance does not improve the VCVPF approximation. It should be pointed out that no matter how many correction terms are added to the potential (2.23), the shear stress evaluated using (2.23) is still non-zero unless $(A + A_1 + A_2 + \cdots) = 0$. Therefore, VCVPF is only an approximation to the exact solution and cannot satisfy the shear stress condition at the free surface.

Prosperetti (1976) considered viscous effects on standing free gravity waves using the same governing equations (2.7) and (2.8) for the viscous correction terms. If we adapt our VCPVF method to treat standing waves represented by the potential $\phi = k^{-1}(\mathrm{d}a/\mathrm{d}t)e^{ky}\cos kx$, we can obtain $-p_v = 2\mu k (\mathrm{d}a/\mathrm{d}t)e^{ky}\cos kx$, which is exactly the same pressure correction obtained by Prosperetti (1976) using a different method.

3. Relation between the pressure correction and Lamb's exact solution

It has been conjectured and is widely believed (Moore 1963; Harper & Moore 1968; Joseph & Wang 2004) that a viscous pressure correction arises in the vortical boundary layer at the free surface which is neglected in the irrotational analysis. However, no viscous pressure correction arises in Lamb's exact solution. His solution is given by a potential ϕ and a streamfunction ψ:

$$u = \frac{\partial\phi}{\partial x} - \frac{\partial\psi}{\partial y}, \quad v = \frac{\partial\phi}{\partial y} + \frac{\partial\psi}{\partial x}, \quad \frac{p}{\rho} = -\frac{\partial\phi}{\partial t} - gy, \tag{3.1}$$

satisfying

$$\nabla^2\phi = 0, \quad \partial\psi/\partial t = \nu\nabla^2\psi. \tag{3.2}$$

The streamfunction gives rise to the rotational part of the flow. No pressure term enters into the streamfunction equation, as we have shown in the previous section that the only harmonic pressure for the rotational part is zero. The pressure p comes

k	p_v/ρ	Term 1	Term 2	Term 3	Term 4
0.01	-2.063×10^{-6}	$-1.325 \times 10^{-9} +$ i2.01×10^{-4}	$-2.063 \times 10^{-6} -$ i2.01×10^{-4}	-1.325×10^{-9}	$5.300 \times 10^{-9} +$ i5.300×10^{-9}
0.1	-2.057×10^{-4}	$-7.441 \times 10^{-7} +$ i0.00358	$-2.071 \times 10^{-4} -$ i0.00358	-7.461×10^{-7}	$2.980 \times 10^{-6} +$ i2.980×10^{-6}
1	-0.02022	$-4.207 \times 10^{-4} +$ i0.06272	$-0.02106 -$ i0.06440	-4.186×10^{-4}	$0.001679 +$ i0.001679
10	-1.881	$-0.3131 + i0.6303$	$-2.423 - i1.513$	-0.1829	$1.038 + i0.8830$

TABLE 1. The value of each term in (3.8) normalized by A^E for SO10000 oil at different wavenumbers; term 1 = $\partial(\phi^J - \phi^E)/\partial t$, term 2 = $g(\eta^J - \eta^E)$, term 3 = $2\nu\partial^2(\phi^J - \phi^E)/\partial y^2$ and term 4 = $2\nu\partial^2\psi^E/\partial x\partial y$.

from Bernoulli's equation in (3.1) and no explicit viscous pressure exists, though p depends on the viscosity through the velocity potential. Lamb shows that (3.2) can be solved with normal modes

$$\phi = A e^{ky} e^{ikx+nt}, \quad \psi = C e^{my} e^{ikx+nt}, \quad m^2 = k^2 + n/\nu, \tag{3.3}$$

where A and C are constants.

It is therefore of interest to derive the connection between the viscous pressure correction p_v in our VCVPF theory and Lamb's exact solution; superscript E represents Lamb's exact solution and J represent Joseph & Wang's VCVPF theory. The irrotational pressure in the two solutions are

$$p^E = -\rho \frac{\partial \phi^E}{\partial t} - \rho g \eta^E, \quad p_i^J = -\rho \frac{\partial \phi^J}{\partial t} - \rho g \eta^J. \tag{3.4}$$

The elevation η is obtained from the kinematic condition at $y \approx 0$

$$\frac{\partial \eta^E}{\partial t} = \frac{\partial \phi^E}{\partial y} + \frac{\partial \psi^E}{\partial x}, \quad \frac{\partial \eta^J}{\partial t} = \frac{\partial \phi^J}{\partial y}. \tag{3.5}$$

The normal stress balance for the two solutions is

$$T_{yy}^E = -p^E + 2\mu \frac{\partial^2 \phi^E}{\partial^2 y} + 2\mu \frac{\partial^2 \psi^E}{\partial x \partial y} = 0, \tag{3.6}$$

$$T_{yy}^J = -p_i^J - p_v + 2\mu \frac{\partial^2 \phi^J}{\partial^2 y} = 0. \tag{3.7}$$

Therefore $T_{yy}^E - T_{yy}^J = 0$ and we can obtain

$$\frac{p_v}{\rho} = \frac{\partial(\phi^J - \phi^E)}{\partial t} + g(\eta^J - \eta^E) + 2\nu \frac{\partial^2(\phi^J - \phi^E)}{\partial y^2} - 2\nu \frac{\partial^2 \psi^E}{\partial x \partial y}. \tag{3.8}$$

The amplitude A for the potential is different in Lamb's exact solution and in VCPVF:

$$\phi^E = A^E e^{nt+ky+ikx}, \quad \phi^J = A^J e^{nt+ky+ikx}, \quad A^E \neq A^J. \tag{3.9}$$

To make the two solutions comparable, we compute the relation between A^E and A^J by equating the dissipation evaluated using Lamb's exact solution and evaluated using VCPVF. Table 1 gives the values of each term in (3.8) normalized by A^E. It seems that the term $g(\eta^J - \eta^E)$ gives the most important contribution to p_v, but the other terms are not negligible.

4. Comparison of the decay rate and wave velocity given by the exact solution, VPF and VCVPF

When the surface tension is ignored, Lamb's exact solution gives rise to the following dispersion relation:

$$n^2 + 4\nu k^2 n + 4\nu^2 k^4 + gk = 4\nu^2 k^3 \sqrt{k^2 + n/\nu}. \tag{4.1}$$

Lamb considered the solution of (4.1) in the limits of small k and large k. When $k \ll k_c = (g/\nu^2)^{1/3}$, he obtained approximately

$$n = -2\nu k^2 \pm ik\sqrt{g/k}, \tag{4.2}$$

which gives rise to the decay rate $-2\nu k^2$, in agreement with the dissipation result, and the wave velocity $\sqrt{g/k}$, which is the same as the wave velocity for inviscid potential flow. When $k \gg k_c = (g/\nu^2)^{1/3}$, Lamb noted that the two roots of (4.1) are both real. One of them is

$$n_1 = -\frac{g}{2\nu k}, \tag{4.3}$$

and the other is

$$n_2 = -0.91\nu k^2. \tag{4.4}$$

Lamb pointed out that n_1 is the more important root because the motion corresponding to n_2 dies out very rapidly.

4.1. *VPF results*

Joseph & Wang (2004) treated this problem using VPF and obtained the following dispersion relation

$$n^2 + 2\nu k^2 n + gk = 0. \tag{4.5}$$

When $k < k_c = (g/\nu^2)^{1/3}$, the solution of (4.5) is

$$n = -\nu k^2 \pm ik\sqrt{g/k - \nu^2 k^2}. \tag{4.6}$$

We note that the decay rate $-\nu k^2$ is half of that in (4.2) and the wave velocity $\sqrt{g/k - \nu^2 k^2}$ is slower than the inviscid wave velocity. When $k > k_c = (g/\nu^2)^{1/3}$, the two roots of (4.5) are both real and they are

$$n = -\nu k^2 \pm \sqrt{\nu^2 k^4 - gk}. \tag{4.7}$$

If $k \gg k_c = (g/\nu^2)^{1/3}$, the above two roots are approximately

$$n_1 = -\frac{g}{2\nu k}, \tag{4.8}$$

and

$$n_2 = -2\nu k^2 + \frac{g}{2\nu k}. \tag{4.9}$$

We note that (4.8) is the same as (4.3), and the magnitude of (4.9) is approximately twice that of (4.4).

4.2. *VCVPF results*

Joseph & Wang (2004) computed a pressure correction and added it to the normal stress balance to obtain

$$n^2 + 4\nu k^2 n + gk = 0, \tag{4.10}$$

Fluid	Water	Glycerine	SO10000	–
$\nu(\mathrm{m^2\,s^{-1}})$	10^{-6}	6.21×10^{-4}	1.03×10^{-2}	10
$k_c\ (\mathrm{m^{-1}})$	21399.7	294.1	45.2	0.461

TABLE 2. The values for the cutoff wavenumber k_c for water, glycerine SO10000 oil and the liquid with $\nu = 10\,\mathrm{m^2\,s^{-1}}$. k_c decreases as the viscosity increases.

which is the dispersion relation for VCVPF theory. When $k < k_c' = (g/4\nu^2)^{1/3}$, the solution of (4.10) is

$$n = -2\nu k^2 \pm \mathrm{i}k\sqrt{g/k - 4\nu^2 k^2}. \tag{4.11}$$

We note that the decay rate $-2\nu k^2$ is the same as in (4.2) and the wave velocity $\sqrt{g/k - 4\nu^2 k^2}$ is slower than the inviscid wave-velocity. When $k > k_c' = (g/4\nu^2)^{1/3}$, the two roots of (4.10) are both real and they are

$$n = -2\nu k^2 \pm \sqrt{4\nu^2 k^4 - gk}. \tag{4.12}$$

If $k \gg k_c' = (g/4\nu^2)^{1/3}$, the above two roots are approximately

$$n_1 = -\frac{g}{4\nu k}, \tag{4.13}$$

and

$$n_2 = -4\nu k^2 + \frac{g}{4\nu k}. \tag{4.14}$$

We note that (4.13) is half of (4.3), and the magnitude of (4.14) is approximately four times that of (4.4).

4.3. *Comparisons for the results*

We compute the solution of (4.1) and compare the real and imaginary part of n with those obtained by solving (4.5) and (4.10). Water, glycerine and SO10000 oil, for which the kinematic viscosity is 10^{-6}, 6.21×10^{-4} and $1.03 \times 10^{-2}\,\mathrm{m^2\,s^{-1}}$, respectively, are chosen as examples. Figures 1 and 2 show the decay rate $-\mathrm{Re}(n)$ for water; the root n_1 when $k > k_c$ is shown in figure 1 and the root n_2 in figure 2. The imaginary part of n, i.e. the wave velocity multiplied by k, is plotted in figure 3 for water. For glycerine and SO10000 oil (figures 4 and 5), we only plot the decay rate corresponding to the more important root n_1; the plots for the root n_2 and the wave velocity are omitted. Figure 6 shows the decay rate corresponding to the root n_1 for $\nu = 10\,\mathrm{m^2\,s^{-1}}$, which is 1000 times more viscous than SO10000 oil; the comparison between the exact solution and VPF, VCVPF is still excellent. The cutoff wavenumber $k_c = (g/\nu^2)^{1/3}$ decreases as the viscosity increases. In Table 2 gives the values of k_c for water, glycerine, SO10000 oil and the liquid with $\nu = 10\,\mathrm{m^2\,s^{-1}}$. In practice, waves associated with different wavenumbers may exist simultaneously. For very viscous fluids, k_c is small and the majority of the wave numbers are above k_c, therefore the motion of monotonic decay dominates; for less viscous fluids, the motion of progressive waves may dominate.

5. Why does the exact solution agree with VCVPF when $k < k_c$ and with VPF when $k > k_c$?

Our VCVPF solution and Lamb's dissipation calculation are based on the assumption that the energy equation (2.17) for the exact solution is approximated
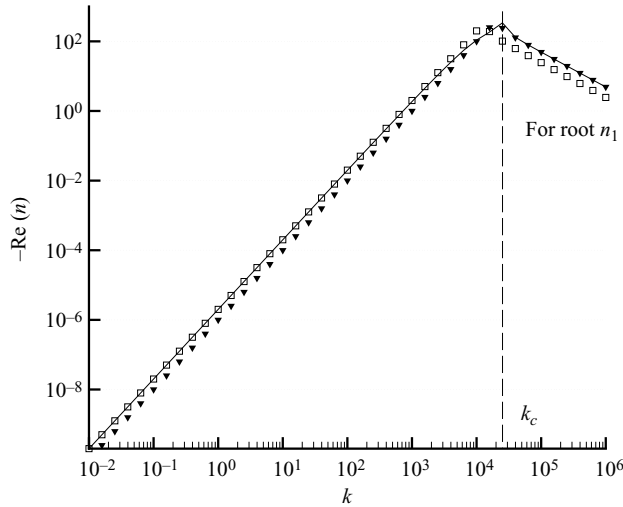
FIGURE 1. Decay rate $-\mathrm{Re}(n)$ *vs.* wavenumber k for water, $\nu = 10^{-6}\,\mathrm{m}^2\,\mathrm{s}^{-1}$. $\mathrm{Re}(n)$ is computed $-$, for the exact solution from (4.1), ▼, for VPF from (4.5) and □, for VCVPF from (4.10). When $k < k_c$, the decay rate $-2\nu k^2$ for VCVPF is in good agreement with the exact solution, whereas the decay rate $-\nu k^2$ for VPF is only half of the exact solution. When $k > k_c$, n has two real solutions in each theory. In this figure, we plot the decay rate n_1 corresponding to (4.3), (4.8) and (4.13). The exact solution can be approximated by $-g/(2\nu k)$; the decay rate $-g/(2\nu k)$ for VPF is in agreement with the exact solution, whereas the decay rate $-g/(4\nu k)$ for VCVPF is only half of the exact solution.
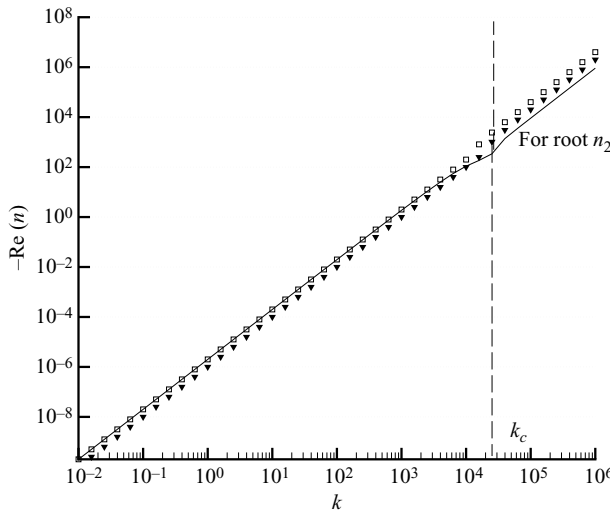
FIGURE 2. Decay rate $-\mathrm{Re}(n)$ *vs.* wavenumber k for water, $\nu = 10^{-6}\,\mathrm{m}^2\,\mathrm{s}^{-1}$. $\mathrm{Re}(n)$ is computed $-$, for the exact solution from (4.1), ▼, for VPF from (4.5) and □, for VCVPF from (4.10). When $k > k_c$, n has two real solutions in each theory. In this figure, we plot the decay rate n_2 corresponding to (4.4), (4.9) and (4.14). The decay rate for the exact solution can be approximated by $-0.91\nu k^2$; the decay rate $\approx -2\nu k^2$ for VPF is closer to the exact solution than the decay rate $\approx -4\nu k^2$ for VCVPF.

well by an irrotational solution. To verify this, we computed and compared the rates of change of the kinetic energy, the potential energy and dissipation terms in (2.17) for Lamb's exact solution and for the purely irrotational part of his solution. The
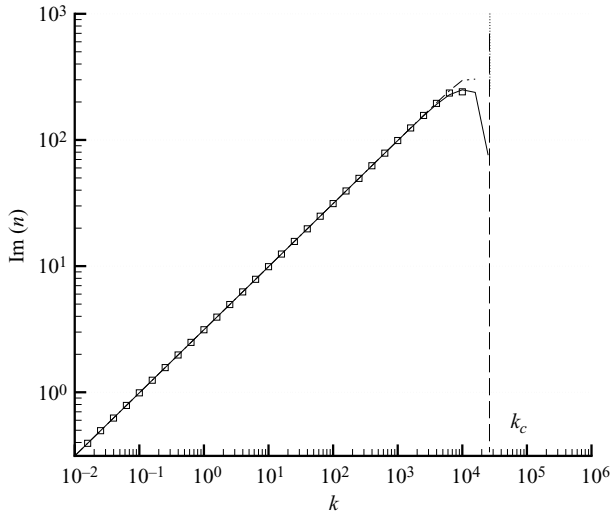
FIGURE 3. $\text{Im}(n)$, i.e. the wave velocity multiplied by k, *vs.* wavenumber k for water, $\nu = 10^{-6}\,\text{m}^2\,\text{s}^{-1}$. $\text{Im}(n)$ is computed –, for the exact solution from (4.1), – - –, for VPF from (4.5) and $\square$, for VCVPF from (4.10). When $k < k_c$, the three theories give almost the same wave velocity. When $k > k_c$, all the three theories give zero imaginary part of n.
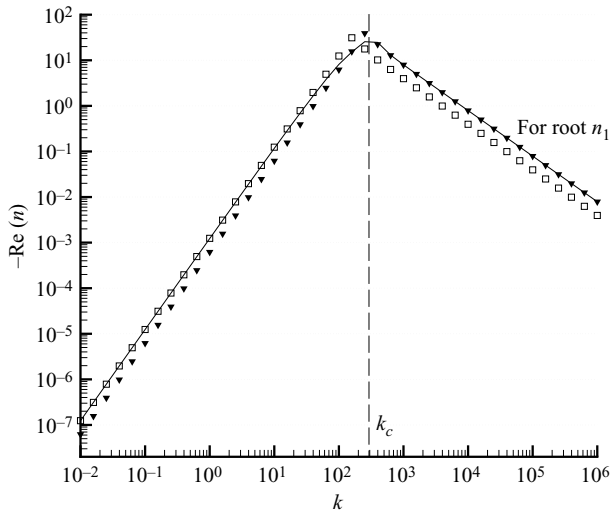

FIGURE 4. Decay rate $-\text{Re}(n)$ *vs.* wavenumber k for glycerine, $\nu = 6.21 \times 10^{-4}\,\text{m}^2\,\text{s}^{-1}$. $\text{Re}(n)$ is computed –, for the exact solution from (4.1), ▼, for VPF from (4.5) and $\square$, for VCVPF from (4.10). When $k < k_c$, the decay rate $-2\nu k^2$ for VCVPF is in good agreement with the exact solution, whereas the decay rate $-\nu k^2$ for VPF is only half of the exact solution. When $k > k_c$, n has two real solutions in each theory. In this figure, we plot the decay rate n_1 corresponding to (4.3), (4.8) and (4.13). The decay rate for the exact solution can be approximated by $-g/(2\nu k)$; the decay rate $-g/(2\nu k)$ for VPF is in agreement with the exact solution, whereas the decay rate $-g/(4\nu k)$ for VCVPF is only half of the exact solution.

agreement is excellent when $k < k_c$. This shows that the vorticity may be neglected in the computation of terms in the energy balance when $k < k_c$, and is consistent with results given in §4 which demonstrate that the decay rates from VCVPF and the dissipation calculation agree with the exact solution when k is small. The agreement
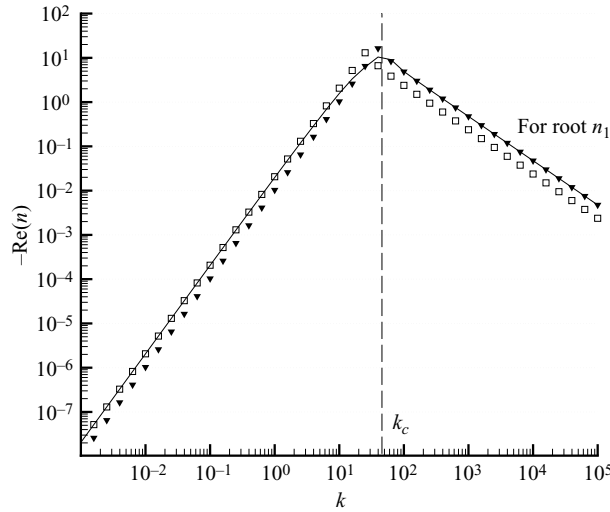
FIGURE 5. Decay rate $-\mathrm{Re}(n)$ *vs.* wavenumber k for SO10000 oil, $\nu = 1.03 \times 10^{-2}\,\mathrm{m}^2\,\mathrm{s}^{-1}$. $\mathrm{Re}(n)$ is computed –, for the exact solution from (4.1), ▼, for VPF from (4.5) and □, for VCVPF from (4.10). When $k < k_c$, the decay rate $-2\nu k^2$ for VCVPF is in good agreement with the exact solution, whereas the decay rate $-\nu k^2$ for VPF is only half of the exact solution. When $k > k_c$, n has two real solutions in each theory. In this figure, we plot the decay rate n_1 corresponding to (4.3), (4.8) and (4.13). The decay rate for the exact solution can be approximated by $-g/(2\nu k)$; the decay rate $-g/(2\nu k)$ for VPF is in agreement with the exact solution, whereas the decay rate $-g/(4\nu k)$ for VCVPF is only half of the exact solution.
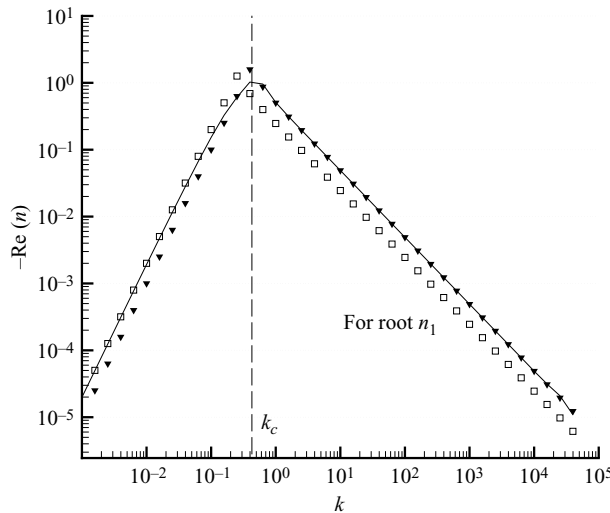

FIGURE 6. Decay rate $-\mathrm{Re}(n)$ *vs.* wavenumber k for $\nu = 10\,\mathrm{m}^2\,\mathrm{s}^{-1}$. $\mathrm{Re}(n)$ is computed –, for the exact solution from (4.1), ▼, for VPF from (4.5) and □, for VCVPF from (4.10). When $k < k_c$, the decay rate $-2\nu k^2$ for VCVPF is in good agreement with the exact solution, whereas the decay rate $-\nu k^2$ for VPF is only half of the exact solution. When $k > k_c$, n has two real solutions in each theory. In this figure, we plot the decay rate n_1 corresponding to (4.3), (4.8) and (4.13). The decay rate for the exact solution can be approximated by $-g/(2\nu k)$; the decay rate $-g/(2\nu k)$ for VPF is in agreement with the exact solution, whereas the decay rate $-g/(4\nu k)$ for VCVPF is only half of the exact solution.

is poor for k in the vicinity of k_c, therefore the decay rates from VCVPF deviate from the exact solution near k_c, as shown in figures 1 to 6.

When k is much larger than k_c, the energy equation is not approximated well by the irrotational part of the exact solution. However, this result does not mean that the vorticity is important. Lamb pointed out $m \approx k$ when k is large, which is confirmed in our calculation. It follows that the vorticity of the exact solution is

$$\nabla^2 \psi = (m^2 - k^2)C\mathrm{e}^{my+ikx+nt} \approx 0; \tag{5.1}$$

the vorticity is negligible when k is large. The result that the wave is nearly irrotational for large k was also pointed out by Tait (1890). Consequently, the decay rate $-g/(2\nu k)$ from VPF is in good agreement with the exact solution and no pressure correction is required.

6. Conclusion

The problem of decay of free gravity waves due to viscosity was analysed using two different theories of viscous potential flow, VPF and VCVPF. The contribution of the viscous part of the normal stress at the gas liquid surface is computed using the potential flow in VPF; otherwise the VPF theory is the same as the irrotational theory of flow of an inviscid fluid. VCVPF is the same as VPF except for an additional viscous contribution to the pressure selected so as to remove the shear stress in the energy balance evaluated using the irrotational flow. The pressure correction leads to a hierarchy of potential flows in powers of viscosity. These higher-order contributions vanish more rapidly than the principal correction which is proportional to μ. The higher-order corrections do not have a boundary-layer structure and may not have a physical significance.

The irrotational theory is in splendid agreement with Lamb's exact solution for all wavenumbers k except for those in a small interval around k_c where progressive waves change to monotonic decay. VCVPF agrees with Lamb's solution when $k < k_c$ (progressive waves) and VPF agrees with Lamb's exact solution when $k > k_c$ (monotonic decay). The cutoff wave number $k_c = (g/\nu^2)^{1/3}$ decreases as the viscosity increases. In practice, waves associated with different wave numbers may exist simultaneously. For very viscous fluids, k_c is small and the majority of the wavenumbers are above k_c, therefore the motion of monotonic decay dominates; for less viscous fluids, the motion of progressive waves may dominate.

There is a boundary layer of vorticity associated with the back and forth motion of the progressive waves. The confined vorticity layer has almost no effect on the solution except for k near k_c. There is no explicit pressure correction in the exact solution. The vortical part of the exact solution does not generate a pressure correction; the pressure depends on the viscosity through the velocity potential and the surface elevation; it is related to the potential and vortical parts of the exact solution in a complicated way. The vortical part is not dominant and the pressure correction is not primarily associated with a boundary layer (see (3.8) and table 1).

The analysis of capillary instability of liquid in gas (Wang, Joseph & Funada 2005) is very much like the analysis of the decay of free gravity waves. The purely potential flow analysis is in excellent agreement with Tomotika's (1935) exact solution which has no explicit dependence on viscous pressure. In the case of capillary instability, the best result is based on VCVPF because the short waves which give rise to a sluggish decay in Lamb's problem are stabilized by surface tension.

REFERENCES

HARPER, J. F. & MOORE, D. W. 1968 The motion of a spherical liquid drop at high Reynolds number. *J. Fluid Mech.* **32**, 367–391.

JOSEPH, D. D. & WANG, J. 2004 The dissipation approximation and viscous potential flow. *J. Fluid Mech.* **505**, 365–377.

KANG, I. S. & LEAL, L. G. 1988 The drag coefficient for a spherical bubble in a uniform streaming flow. *Phys. Fluids* **31**, 233–237.

LAMB, H. 1932 *Hydrodynamics*, 6th edn. Cambridge University Press. (Reprinted by Dover, 1945).

MOORE, D. W. 1963 The boundary layer on a spherical gas bubble. *J. Fluid Mech.* **16**, 161–176.

PROSPERETTI, A. 1976 Viscous effects on small-amplitude surface waves. *Phys. Fluids* **19**, 195–203.

TAIT, P. G. 1890 Note on ripples in a viscous liquid, *Proc. R. Soc. Edin.* **17**, 110 [*Scientific Papers*, Cambridge University Press, 1898–1900, vol. 2, p. 313].

TOMOTIKA, S. 1935 On the instability of a cylindrical thread of a viscous liquid surrounded by another viscous fluid. *Proc. R. Soc. Lond.* A **150**, 322–337.

WANG, J., JOSEPH, D. D. & FUNADA, T. 2005 Pressure corrections for potential flow analysis of capillary instability of viscous fluids. *J. Fluid Mech.* **522**, 383–394.